Springer

KSME

Journal of Mechanical Science and Technology 31 (1) (2017) 189~196
www.springerlink.com/content/1738-494x(Print)/1976-3824(Online)
DOI 10.1007/s12206-016-1221-3

Experimental investigation of a supercritical airfoil boundary layer in pitching motion †

Mehran Masdari[1,*], Mohsen Jahanmiri[2], Mohammad Reza Soltani[3], Arshia Tabrizian[1] and Mohammad Gorji[2]

[1]*Faculty of New Science and Technology, University of Tehran, Tehran, Iran*
[2]*Department of Mechanical and Aerospace Engineering, Shiraz University of Technology, Shiraz, Iran*
[3]*Department of Aerospace Engineering, Sharif University of Technology, Tehran, Iran*

(Manuscript Received October 29, 2015; Revised June 25, 2016; Accepted August 18, 2016)

Abstract

In this study, the boundary layer velocity profile on the upper surface of a supercritical airfoil in a forced sinusoidal pitching motion was measured and experimentally investigated. Measurements were performed using a boundary layer rake, including total pressure tubes positioned at 25 % of the chord far from the leading edge on the upper surface. For static measurements, the effects of the angle of attack between −3° and 14° and free-stream velocity between 40 $\frac{m}{s}$ and 70 $\frac{m}{s}$ were investigated; for dynamic measurements, the effects of oscillation amplitude variation between ±3° and ±10°, reduced frequency from 0.007 to 0.0313, and mean angle of attack between −3° and 6° were studied during one oscillation cycle. Results indicated that the boundary layer thickness decreased in upstroke motion. Increasing the oscillation frequency led to the extension of hysteresis loops. Fast Fourier transform was used on pressure signals to study the amplitude of the dominant frequency in the velocity profile. Spectral analysis showed that the dominant forced frequency of oscillation in the boundary layer and the amplitude of this frequency were varied by increasing the reduced frequency and other parameters.

Keywords: Unsteady boundary layer; Pitching motion; Supercritical airfoil; Hysteresis; Dominant frequency

1. Introduction

Studying flow behavior around plane propellers, rotor blades of helicopters, wind turbines, and highly maneuverable wings of aircraft is significant. In most cases, forces produced by an unsteady airflow are considerably higher than those produced in a steady flow. Therefore, the effects of unsteadiness should not be disregarded.

Since the early 20th century, studies have focused on airflow around lifting surfaces. Given the limitations caused by insufficient experimental, numerical, and analytical instruments, simplifications are mostly applied, which ignore unsteady sources. Several older studies are listed in Refs. [1-11].

In 1988, Car conducted extensive research on the analysis and calculation (prediction) of dynamic stall [12]. Kouchesfahani (1989) studied the effect of sinusoidal and non-sinusoidal waves on an airfoil during pitch oscillation with a small amplitude through the vortex structure of the wake. He determined the mean flow velocity in the flow direction by visualizing the flow and conducting numerical analyses using the laser Doppler velocimetry technique. Kouchesfahani reported that fair control might be exercised over the wake structure by maintaining the frequency, amplitude, and oscillating wave form under control. In addition, he showed that in the case of a high reduced frequency, the wake turned into a jet-like flow, followed by thrust production [13]. In 1998, Ti-Li and Baso performed an experimental study related to a developed unsteady boundary layer on an oscillating airfoil by utilizing hot film sensors. In their study, a NACA-0012-type airfoil was selected, and sinusoidal oscillation was measured by 140 points [14]. In 2003, Leo identified the profile of the boundary layer in torsional motion when transition occurred. The presented data provided a good qualitative approximation of the boundary layer. In the same year (2003), Chitoberri and Elright applied a universal function, in which the wake effects were considered in an unsteady boundary layer to model the transition state. The presentation of a dotter model contributed to predicting the behavior of the boundary layer, such as shear stress and heat transfer, and led to the development of numeri-

*Corresponding author. Tel.: +98 9126219381, Fax.: +98 21 88056527
E-mail address: m.masdari@ut.ac.ir
† Recommended by Associate Editor Kyu Hong Kim

cal algorithms [15]. Gopalan (2008) conducted a numerical analysis on micro flyers and achieved a noteworthy and reliable result, namely, a code that was applicable to both pitching and translational motions. The disadvantages of this code include its limitation in laminar flow, its inapplicability to Reynolds numbers higher than 80000, and the failure to consider transition in its solution [16]. In 2009, Kong performed a numerical study on the translational and rotational oscillations of an airfoil within Reynolds numbers ranging from 10000 to 60000 and validated the achieved code through particle image velocimetry tests. This code also predicted the results for laminar flow [17]. In 2010, Ghanbari et al. conducted a study on the effects of the unsteady parameters of flow on the aerodynamics of a pitching airfoil in small Reynolds numbers through a numerical method (limited mass) [18]. In the same year, Liang et al. performed a numerical simulation based on the third- and fourth-order spectral difference method and a non-uniform grid on an airfoil during pitching and plunging oscillations [19]. In 2011, Fang et al. investigated the boundary layers of an unsteady incompressible stagnation-point flow with mass transfer. In this study, the similarity transformation technique was adopted, and the similarity equation was solved using numerical methods [20]. In 2015, Zheng and Ghate applied a solution procedure based on two-parameter asymptotic expansions in terms of a Blasius parameter and dimensionless time; this solution was presented for a 2D, unsteady boundary layer over a flat plate [21]. Haghiri et al. studied the characteristics of the boundary layer, and the transition region was experimentally investigated through statistical methods. Results showed that in the shock-free case, the boundary layer regions were identifiable via statistical analysis, such as root mean square and skewness, as in incompressible flow [22]. In 2016, instabilities arising in unsteady boundary layers with reverse flow were experimentally investigated by Das et al. [23].

Although extensive research has been conducted in this field, numerous shortcomings have been observed in studies regarding unsteady boundary layers, particularly in turbulent flows. The effects of various quantities of flow on the unsteady boundary layer should be investigated because these effects have not yet been defined. Given the lack of sufficient practical information on supercritical airfoils, the effects of flow on the boundary layer profile for any design process should be evaluated. Therefore, static and dynamic tests should be conducted to examine the effects of unsteady parameters on the efficiency of airfoils. The present study aims to verify the dependency of boundary layer thickness on the reduced frequency and amplitude of pitching motion.

2. Instruments and test methods

Experiments were conducted in a low-speed, closed-circuit wind tunnel with a rectangular test section of 80×80×200 cm^3. The test section speed varied continuously from 10 m/s to 100 m/s at Reynolds numbers of up to 1.2×10^6. The tunnel inlet had a contraction ratio of 7:1, with four large, anti-turbulence screens and a honeycomb in front of the contraction to reduce tunnel turbulence intensity to less than 0.2 % in the test section at all speeds [24]. Fig. 1 shows a general view of the wind tunnel.

Fig. 1. Overall view of the wind tunnel used in the experiment.

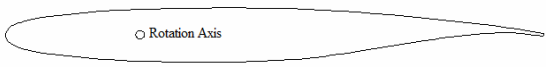

Fig. 2. Section of the supercritical airfoil.

The model was a supercritical airfoil, which had a 30 cm chord and an 80 cm span made of PVC with a metal core. A steel axis was devised within the model at a quarter of the chord away from the leading edge to generate pitching oscillation. Fig. 2 presents the section of the supercritical airfoil (SC-410).

A rake with small pitot pressure tubes (0.6 mm in diameter) was used to measure the pressure distribution, and consequently, the velocity distribution of the boundary layer. This rake was completely attached to the model surface.

Pressure transducers, with an excitation voltage of 8-16 V, an output voltage of 1-6 V, a pressure range of ±1 psi, and a response time of 1 ms, were used. The output voltage was transferred to a 12-bit, 64-channel analog-to-digital data acquisition board.

An AC electromotor with a crank system was applied to generate sinusoidal pitching motion. The frequency of motion could be adjusted by changing the frequency of rotation of the electromotor via an inverter. The amplitude of rotation was varied linearly by changing the length of the crank link.

A digital pulse counter was used to measure and monitor the instantaneous angle of attack. The analog output of this counter was introduced into the A/D board as an external trigger.

The model, through its shaft and rake, was fastened onto an

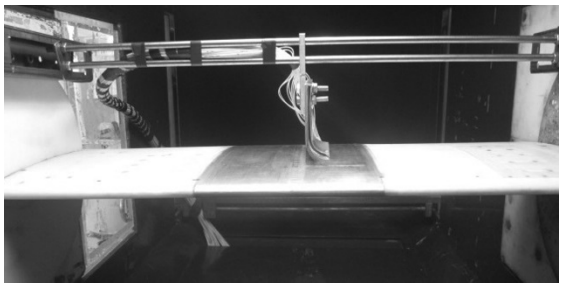

Fig. 3. Front view of the model and the rake in the test section.

interface circular plate on the tunnel wall. The interface plate was attached to the rotary system, which was located behind the tunnel wall. Consequently, the crank system rotated the interface plate, rake, and model together. Fig. 3 shows the position of the model and the rake in the test section.

Data were collected by placing a pressure rake on the airfoil surface and connecting the pitot pressure tubes of the rake to the transducers during oscillation.

The model and the rake were attached to two rotary plates, such that they were fixed to each other but oscillating together to create oscillating motion.

Two types of tests (static and dynamic) were conducted. In the static tests, the angle of attack and the free-stream velocity were the adjustable parameters during oscillation; in the dynamic tests, the amplitude of oscillation, reduced frequency, and mean angle of attack were the adjustable parameters.

The authors used the equation introduced in Ref. [25] to consider the uncertainty in the velocity profile of the boundary layer and to disregard the measurement and linearity errors of the sensors. Bios error and method precision were the most important sources of errors in the experimental studies. Uncertainty analysis was performed in the boundary layer problem using the following equation:

$$\frac{B_u}{u}=\sqrt{(\frac{B_{\Delta v}}{2\Delta v})^2+(\frac{B_\rho}{2\rho})^2+(\frac{B_s}{2s})^2}\ ,$$

where $B_{\Delta v}$ is the maximum error produced by the electronic devices, B_ρ is the maximum error generated via the density changes during the test, B_S is the maximum error of the calibration slope, Δv is the voltage change, ρ is the density, and S is the calibration slope.

The maximum calculated error using the preceding formula at a velocity of 50 m/s was approximately 5 %.

3. Test results

The static condition results are first discussed in this section, followed by the dynamic condition results. In all the tests, total pressure was measured using the boundary layer rake, and velocity profile was calculated using total and static pressures. Static pressure was assumed to be nearly constant across the boundary layer.

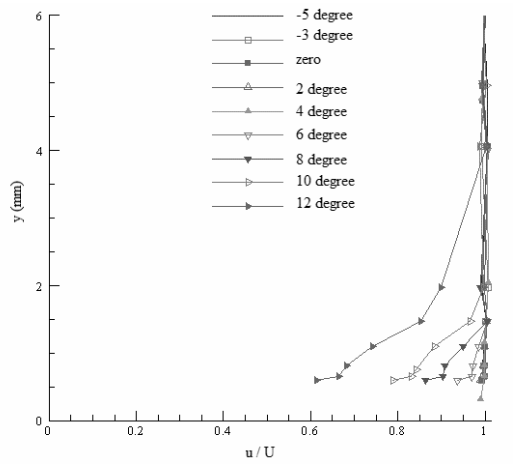

Fig. 4. Boundary layer profile at 25 % chord in 50 m/s.

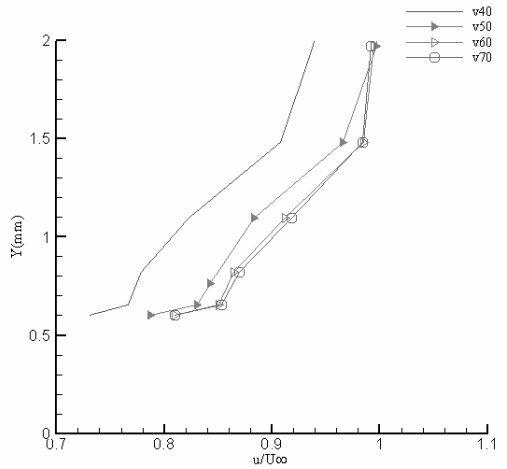

Fig. 5. Boundary layer profile at 25 % chord and 10°.

3.1 Static test results

All data were acquired via the boundary layer rake positioned on the upper surface of the airfoil with a distance of 1/4 chord from the leading edge. In all the cases, free-stream velocity was varied between 40 m/s and 70 m/s, and the angle of attack was varied from −5° to 12°.

Given the wall thickness of the rake tube, the closest point of the velocity profile to the surface was located at 0.6 mm far from the surface in figures.

Fig. 4 shows the boundary layer profile for angles of attack of −5° to 12° at a velocity of 50 m/s. The boundary layer did not increase significantly in angles of attack less than 5°. This slight increase might be attributed to airfoil geometry because supercritical airfoils were slightly curved on the top, which caused an insignificant pressure gradient, and consequently, minimized boundary layer growth. Therefore, the pressure tubes could not detect any remarkable change in pressure. For other velocities, the boundary layer also exhibited the same behavior.

Fig. 5 illustrates the boundary layer profile at various free-

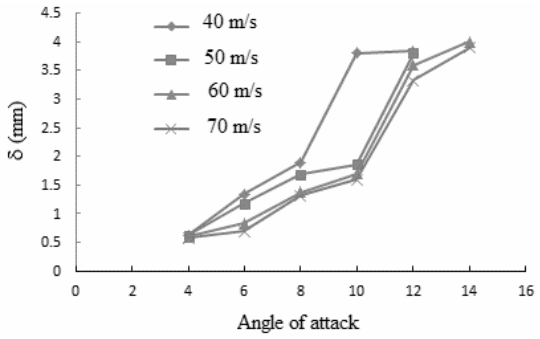

Fig. 6. Boundary layer thickness vs. angle of attack.

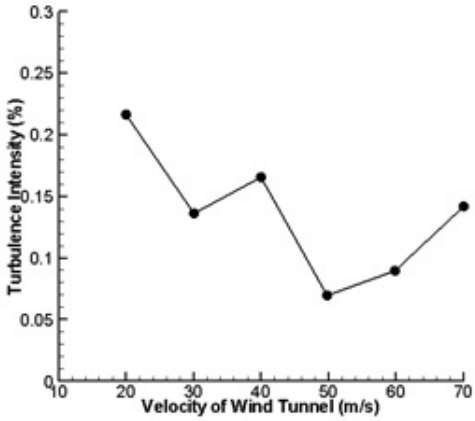

Fig. 7. Wind tunnel turbulence intensity.

stream velocities and an angle of attack of 10°. As velocity increased, boundary layer thickness decreased. The velocity increase would provide considerable energy to flow and caused the later separation.

Fig. 6 shows the boundary layer thickness versus the angle of attack under different velocities. As indicated in the figure, increasing the angle of attack led to an increase in the thickness of the boundary layer under all velocities, whereas increasing the velocity led to a decrease in the thickness of the boundary layer for all the angles of attack.

The increase in boundary layer thickness at velocities of 40 m/s and 50 m/s might be related to the turbulence intensity behavior at these velocities in the wind tunnel test section. As shown in Fig. 7, the turbulence intensity at a velocity of 40 m/s was higher than the others.

3.2 Dynamic test results

An extensive experimental investigation was conducted on an oscillating airfoil in pitching motion over a range of reduced frequencies, k = 0.007 to 0.031, and various oscillation amplitudes. The boundary layer on the upper surface of the airfoil at one quarter of the chord was measured at Reynolds numbers 0.78×10^6.

Fig. 8 depicts the samples of the velocity signals for seven pitot tubes of the boundary layer rake when the maximum

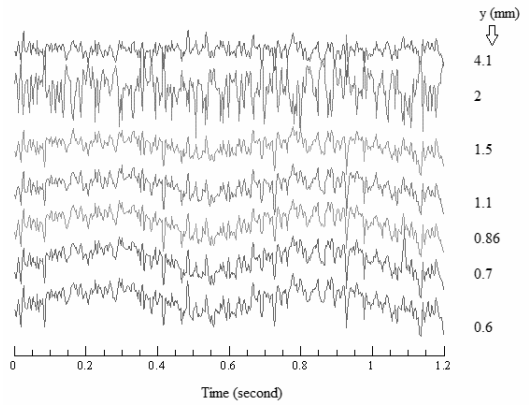

Fig. 8. Instantaneous velocity vs. time (K = 0.0313, d = ±10, α0 = 2).

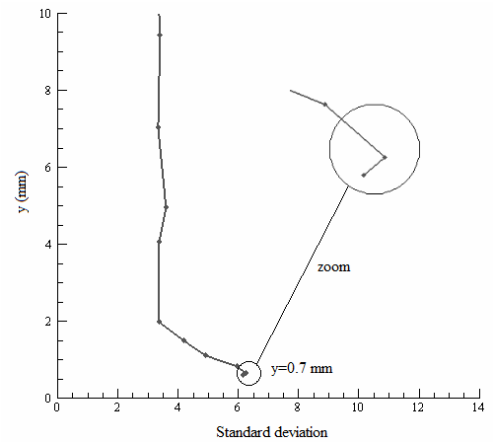

Fig. 9. Standard deviation graph for K = 0.0313, d = ± 10 and α0=2.

angle of attack is near the static stall angle and the mean angle of attack is zero. As shown in the figure, velocity fluctuations continued up to a height of 1.5 mm above the airfoil surface.

Standard deviation was adopted to determine the point that underwent the most turbulent flow field. In Fig. 9, the point with the highest standard deviation in the oscillating mode was found to be 0.7 mm far from the airfoil surface.

The dominant frequency was calculated at the most turbulent point via Fourier transform to determine the extent to which airflow in the boundary layer was affected by airfoil oscillation.

Fig. 10 illustrates a sample of the Fast Fourier transform (FFT) for a position in the boundary layer with the maximum standard deviation. The largest amplitude belonged to the oscillation frequency of 1.7 Hz, which corresponded to the reduced frequency of 0.0313. Therefore, the turbulence generated in the flow by airfoil motion permeated into the boundary layer.

An oscillation period was divided into eight equal parts to analyze the instantaneous boundary layer profile and to avoid a large mass of data. Fig. 11 and all the subsequent figures were studied using these intervals.

Fig. 12 presents a sample of the boundary layer profile, with

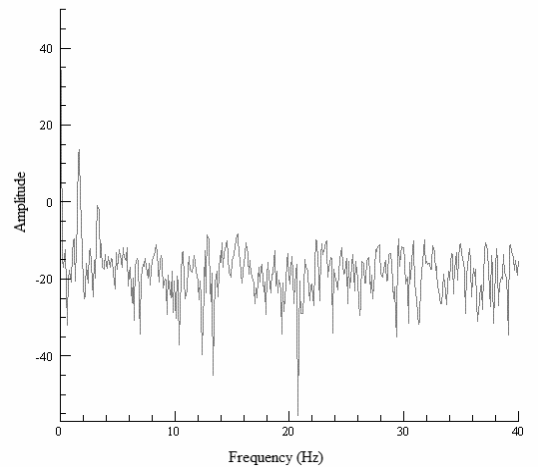

Fig. 10. FFT for K = 0.0313, d = ±10 and α0 = 2.

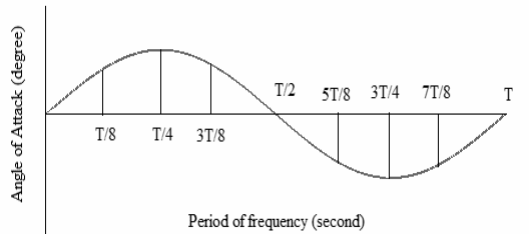

Fig. 11. Divided period of oscillation to T/8.

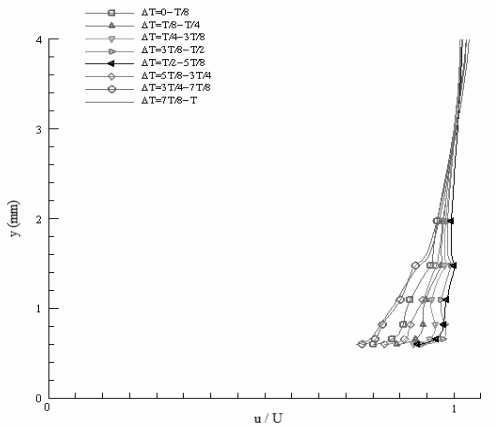

Fig. 12. Velocity boundary layer at a free-stream velocity of 50 m/s in T/8 for K = 0.0313, d = ±10 and α0 = 2.

a reduced frequency of 0.0313, an oscillation amplitude of 10°, and a mean angle of 2°. As the figure illustrates, the boundary layer growth in the upstroke motion of the airfoil has a steeper gradient than that in the downstroke motion.

Fig. 13 illustrates the boundary layer thickness. As shown in the figure, a difference exists between the thickness of the boundary layer in upstroke and downstroke motions at each reduced frequency. This difference creates hysteresis loops in one oscillation period. During an upstroke motion, the thickness of the boundary layer decreases.

Fig. 14 shows the amplitude of the dominant frequency in FFT versus oscillation amplitudes of ±3°, ±5° and ±10° for

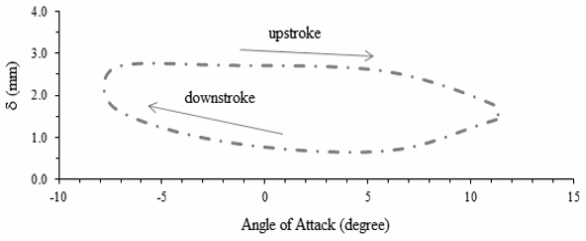

Fig. 13. Boundary layer thickness vs. instance angle of attack at a free-stream velocity of 50 m/s for K = 0.0313, d = ±10 and α0 = 2.

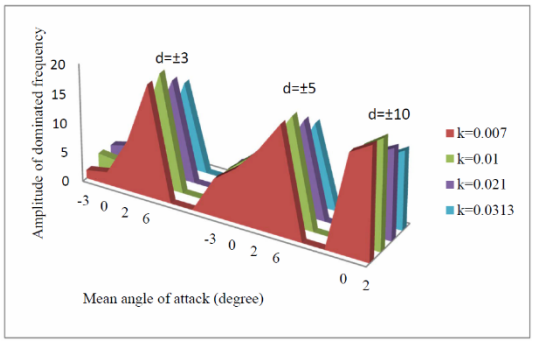

Fig. 14. Amplitude of dominant frequency vs. mean angle of attack.

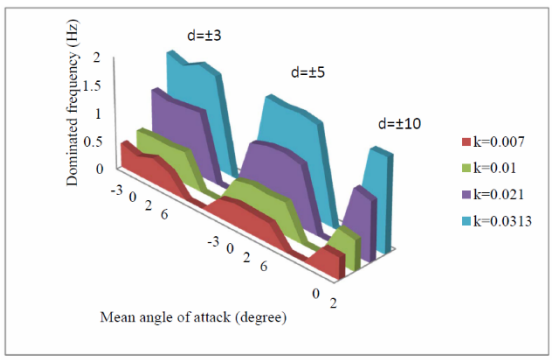

Fig. 15. Dominant frequency vs. mean angle of attack.

various mean angles of attack at different reduced frequencies. As shown in this figure, the amplitude of dominant frequency does not change significantly with the mean angle of attack. The oscillation amplitude is the most important criterion that influences perturbation on the boundary layer. Therefore, increasing the mean angle of attack has no influence on perturbation. By contrast, increasing reduced frequency reduces the amplitude of the dominant frequency. In all the oscillation frequencies, when the angle of attack is greater than zero, an increase in the oscillation frequency leads to a decrease in the amplitude of FFT. In addition, an increase in oscillation amplitude causes gentle gradient of changes. At mean angles of attack of −3°, 0° and 2°, the amplitude of FFT increases; at a mean angle of attack of 6°, it does not change significantly. At higher angles of attack, the vortices do not enter the boundary layer from the leading edge.

In Fig. 15, the dominant frequency in the FFT versus oscillation amplitude in angles of attack of −3°, 0° and 6° is pre-

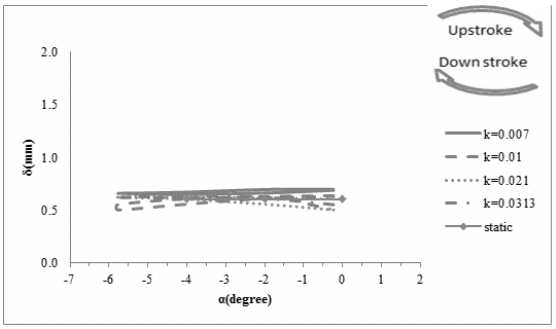

Fig. 16. Change in boundary layer thickness vs. instance angle of attack for d = ±3 and α0 = −3 at 25 % chord.

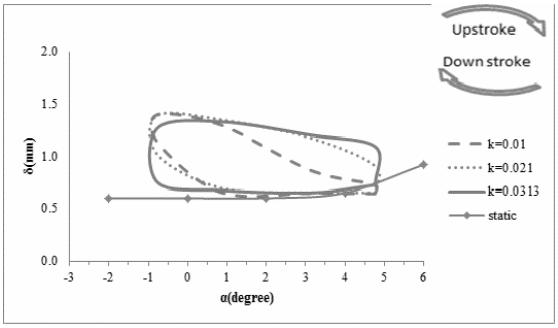

Fig. 17. Change in boundary layer thickness vs. instance angle of attack for d = ±3 and α0 = 2 at 25 % chord.

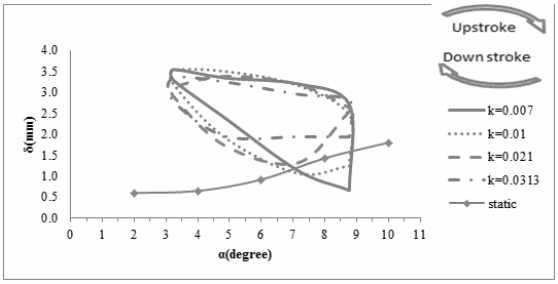

Fig. 18. Change in boundary layer thickness vs. instance angle of attack for d = ±3 and α0 = 6 at 25 % chord.

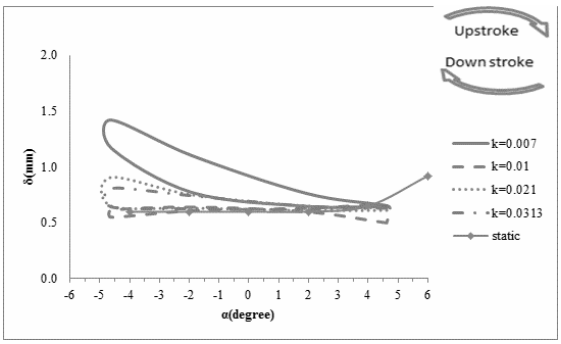

Fig. 19. Change in boundary layer thickness vs. instance angle of attack for d = ±5 and α0 = 0 at 25 % chord.

sented. The mean angle of attack has no effect on the amplitude of the dominant frequency range, whereas the oscillation frequency has a major effect on the amplitude of the dominant frequency range. That is, the boundary layer exhibits higher sensitivity to oscillation frequency.

The chart illustrated in Fig. 16 shows the boundary layer thickness versus the angle of attack. The oscillation amplitude is 3° for a mean angle of attack of −3, and different reduced frequencies are discussed. Neither the change in the thickness of the boundary layer nor the growth of the boundary layer at the aforementioned oscillation amplitude and mean angle of attack is significant. This result is attributed to the presence of a negative angle of attack during most of the oscillation period. The measurement of the boundary layer is restricted by the measuring instrument because the boundary layer in this condition is extremely thin. No growth of the boundary layer is observed in most cases, which have negative angles of attack independent of the amplitude and frequency of motion.

The boundary layer thickness versus the angle of attack in a complete oscillation period with an amplitude of 3° for a mean angle of attack of 2° is presented in Fig. 17. The figure shows that the difference between boundary layer thickness in the upstroke and downstroke motions causes the formation of hysteresis loops. This phenomenon occurs as a result of a phase lag caused by low time scales in the boundary layer. Hence, as the reduced frequency increases, the hysteresis loops widens, and consequently, lag is increased in the boundary layer. In addition, boundary layer thickness in the upstroke motion is less than that in the downstroke motion. In both phases, however, thickness is more than that in the static mode because of the apparent mass transferred in the dynamic case.

Fig. 18 shows the boundary layer thickness versus the angle of attack in a motion with an amplitude of 3° at a mean angle of attack of 6°. In comparison with the previous graph, a larger difference in thickness is observed because of the increase in the angle of attack. In the two reduced frequencies of 0.007 and 0.01 and an angle of 7°, the thickness of the boundary layer in the upstroke mode is more than the static value; in the downstroke mode, the thickness is less than the static value. This result is attributed to the apparent mass transferred in dynamic motion, which is absent in the static test.

As shown in Fig. 19, the variation in the boundary layer thickness in an oscillation with an amplitude of 5° for 0 mean angle of attack, leads to the formation of hysteresis loops during the motion. In the upstroke motion, an increase in the angular moment causes the thickness of the boundary layer to decrease. This decrease reaches the greatest value when the reduced frequency is 0.007.

The boundary layer thickness versus the angle of attack in the pitching motion with an amplitude of 10° for 0 mean angle is shown in Fig. 20. At a reduced frequency of 0.007, narrower loops are formed compared with those in the other three reduced frequencies. This result indicates that as oscillation amplitude increases, the volume of the apparent mass and this parameter are introduced by the reduced frequencies and widened the hysteresis loops.

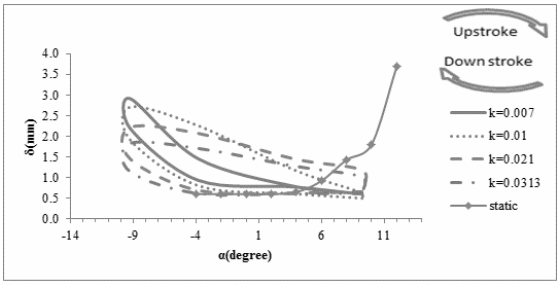

Fig. 20. Change in boundary layer thickness vs. instance angle of attack for d = ±10 and α0 = 0 at 25 % chord.

4. Conclusions

The boundary layer of a supercritical airfoil under the effect of sinusoidal pitching motion was investigated by measuring total pressure in the boundary layer. The results of the static studies showed that boundary layer thickness increased as the angle of attack increased. For angles of attack less than 4°, no measurable effect was observed on the boundary layer that could be attributed to the measurement method. Spectral analysis indicated that the oscillation frequency was the most dominant frequency within the boundary layer.

For dynamic tests, the spectral analysis showed that the sensitivity of the oscillation amplitude was a function of oscillation frequency, and the oscillation amplitude of the airfoil did not have significant effects on the pressures measured at the boundary layer.

A higher mean angle of attack of the airfoil forced the boundary layer to be more under the influence of the oscillating motion of the airfoil, and a wider hysteresis loop was formed.

The changes in the thickness of the boundary layer were nearly imperceptible in angles 0° and −3°, with all the frequencies and amplitudes of oscillation.

All the dynamic results implied that the thickness of the boundary layer in one oscillation cycle decreased in the upstroke motion and increased in the downstroke motion of the airfoil.

For angles of attack of approximately 6° or greater, the boundary layer thickness was less than its value in the static test. This result was attributed to the effect of the apparent mass and phase lag, which was generated in dynamic motion. The flow was still before the dynamic stall zone.

Acknowledgment

The tests in this study would have been impossible to conduct without the support and contributions of Mr. Hossein Shirvani. Therefore, we would like to express our gratitude and appreciation to him.

Nomenclature

T : Period of time

α_0 : Mean angle of attack

f : Frequency of oscillation

c : Chord

U_∞ : Free-stream velocity

$k = \frac{\pi fc}{u_\infty}$: Reduced frequency

References

[1] R. Knoller, Die gesetze des luftwiderstands, *FlugundMotorechnik (Wien)*, 3 (21) (1909) 1-7.

[2] A. Betz, Ein betragzur erkl aerungdessegelfluges, *Z. f. Flugtechnikund Motorlutschiffahrt*, 3 (1912) 269-272.

[3] W. Birnbaum, Der Schlagflügelpropeller und die kleinen Schwingungenelastischbefestigter Tragflügel, *Zeitschriftfür-Flugtechnik und Motorluftschiffahrt*, 15 (1924) 128-134.

[4] T. Theodersen, General theory of aerodynamic instability and mechanism of flutter, *NACA Rept*., 496 (1935).

[5] T. Von Karman and J. M. Burgers, *General aerodynamic theory perfaet fluid*, Aerodynamic Theory, Edited by W. F. Durand, Division E, Julius-Springer, Berlin, 2 (1943) 308.

[6] J. B. Bratt, Flow patterns in the wake of an oscillating airfoil, *Aeronautical Research Council,* R&M 2773 (1950).

[7] J. Lighthill, *Aerodynamic aspects of animal flight, swimming and flying in nature*, New York: Plenum Press, II (1970) 423-491.

[8] D. P. Telionis, D. Th. Tsahalis and M. J. Werle, Numerical investigation of unsteady boundary-layer separation, *Physics of Fluids*, 16 (8) (1973-1974) 968-973.

[9] W. R. Sears and D. P. Telionis, Boundary-layer separation in unsteady flow, *SIAM Journal on Applied Mathematics*, 28 (1) (1975) 215-235.

[10] W. J. McCroskey, Unsteady airfoils, *Annual Review Fluid Mechanics,* 14 (1982) 285-311.

[11] W. Carr and I. T. Cebec, Calculation of boundary layers of oscillating airfoils, *USAAVSCOM Technical Report 84-A-1* (1985).

[12] L. W. Carr, Progress in analysis and prediction of dynamic stall, *Journal of Aircraft,* 25 (1) (1988) 6-17.

[13] M. M. Koochesfahani, Vortical pattern in the wake of an oscillating airfoil, *AIAA Journal*, 27 (1989) 1200-1205.

[14] K. D. Jones, C. M. Dohring and M. F. Platzer, Experimental and computational investigation of the Knoller-Betz effect, *AIAA Journal*, 36 (7) (1998) 1240-1246.

[15] M. T. Schobeiri and L. Wright, Advances in unsteady boundary layer transition research, Part II Experimental Verification, *International Journal of Rotating Machinery*, 9 (1) (2003) 11-22.

[16] H. Gopalan, Numerical modeling of aerodynamics of airfoils of micro air vehicles in gusty environment, *Ph.D. Thesis,* University of Akron (2008).

[17] C.-K. Kang and Y. S. Baik, Fluid dynamics of pitching and plunging airfoils of Reynolds number between 1×104 and 6×104, *47th AIAA Aerospace Sciences Meeting Including The New Horizons Forum and Aerospace Exposition Or-*

lando, Florida (2009).

[18] H. Alighanbari, M. R. Amiralaei and S. M. Hashemi, An investigation into the effects of unsteady parameters on the aerodynamics of a low Reynolds number pitching airfoil, *Journal of Fluids and Structures,* 26 (2010) 979-993.

[19] C. Liang, K. Ou, S. Premasuthan, A. Jameson and Z. J. Wang, High-order accurate simulations of unsteady flow past plunging and pitching airfoils, *Journal Computers & Fluids*, 40 (2011) 236-248.

[20] T. Fang, C. F. Lee and J. Zhang, The boundary layers of an unsteady incompressible stagnation-point flow with mass transfer, *International Journal of Non-Linear Mechanics*, 46 (7) (2011) 942-948.

[21] Z. C. Zheng and A. S. Ghate, A solution of two-parameter asymptotic expansions for a two-dimensional unsteady boundary layer, *Applied Mathematics and Computation*, 270 (2015) 90-104.

[22] A. A. Haghiri, N. Fallahpour, M. Mani and M. Tadjfar, Experimental study of boundary layer in compressible flow using hot film sensors through statistical and qualitative methods, *Journal of Mechanical Science and Technology*, 29 (11) (2015) 4671-4679.

[23] S. P. Das, U. Srinivasan and J. H. Arakeri, Instabilities in unsteady boundary layers with reverse flow, *European Journal of Mechanics - B/Fluids*, 55 (1) (2016) 49-62.

[24] K. Ghorbanian, M. R. Soltani and M. D. Manshadi, Experimental investigation on turbulence intensity reduction in subsonic wind tunnels, *Aerospace science and Technology*, Elsevier (2010).

[25] T. G. Beckwith, R. D. Maraugoni and J. H. V. Lienhard, *Mechanical Measurements*, Fifth Edition, Addison-Wesley Publishing Company (1993) 45-115.

Mehran Masdari is an Assistant Professor at the New Sciences and Technologies Department of Tehran University. He obtained his B.Sc. in Aerospace Engineering, M.Sc. in Aerodynamics, and Ph.D. in Aerodynamics from the Sharif University of Technology in Tehran, Iran in 2000, 2003, and 2011, respectively. His research interests include applied aerodynamics, wind tunnel testing, neural network, and data processing.